



Target-centric angle variables in pursuit tracking

Tim Eakin¹ 

Received: 22 February 2020 / Accepted: 19 June 2020 / Published online: 5 July 2020
© Springer Nature Switzerland AG 2020

Abstract

A method for constructing a dynamic local reference frame centered at the location of a pursuit target is proposed. It uses original fixed reference frame coordinates for three positions: the location of a moving target, the location of a pursuing entity, and a third reference point that defines the instantaneous target trajectory direction. The method involves rigid body geometric operations and creates a consistent local reference frame configuration having its origin at the target location. The local frame also has the target trajectory pointing in the positive x axis direction, and a defined azimuth plane descriptive of the current pursuer location. This plane is determined by a concluding local frame rotation around the set x axis, which specifies a particular y axis direction. If the pursuer position is not on the local frame's azimuth plane, its perpendicular projection on to that plane serves as an additional position for use in defining angle variables. Three angle variables relevant to the pursuit dynamics (not all mutually independent) are obtained from the three coordinate values of the pursuer position in the local frame: an elevation angle, an azimuth angle, and a bearing angle that basically describes how far off course the pursuer position is from being directly behind the target's current trajectory path position. To illustrate the method of obtaining these angles and to demonstrate their potential usefulness in characterizing pursuit behavior, example experimental data from a motor control and coordination pursuit task performance are presented and analyzed.

Keywords Tracking · Angles · Motor performance · Assessment metric

1 Introduction

Pure pursuit tracking refers to a dynamical system consisting of two objects: an entity being pursued (the “target”), which constantly moves with respect to a fixed global reference frame; and a pursuing entity (the “pursuer”), which has the objective of trying to reach and acquire the target position. Details can vary according to the situation. In some cases the pursuit event terminates once the pursuer first reaches the target, but in many research settings the target moves along a predetermined path over a predetermined time interval and the pursuer attempts to maintain a position as close to the target as possible throughout the duration of the event. If the pursuer is a human or other being capable of formulating

a conscious pursuit strategy it will have proprioceptive awareness of its own position and momentum and attention will be focused on the perceived position and momentum of the target. Thus, a remote static origin of an external reference frame is not a particularly useful location for the pursuer to utilize in making angular adjustments of its own movements in response to changes in the target position along its trajectory. A dynamic reference frame with the target and vertices of pursuit characterization angles at the origin is therefore more appropriate and useful in evaluating the behavior and performance of the pursuer.

The potential for application and use of pursuit tracking systems is very general and can occur in various settings and in quite diverse contexts. Many have no direct

✉ Tim Eakin, eakin@austin.utexas.edu | ¹Department of Kinesiology and Health Education, The University of Texas at Austin, Austin, TX 78712-1415, USA.



connection to biological phenomena, such as controlling autonomous vehicles[1] or interception of projectiles[2]. However, many experimental research applications involve biological systems. Within the biological realm there is a substantial diversity of areas for which pursuit tracking is a useful tool. A few examples demonstrate the broad utility of pursuit tracking in the context of biological studies. It has been used as one component of multitasking in assessing executive function in working memory[3], for characterizing ocular saccades in vision research[4], as a clinical tool in assessing motor learning in patients with a neurological deficit[5], in characterizing abrupt changes in fingertip force production modulation[6], as well as for developing and testing perceptual control theory models of motor behavior[7]. Our particular interest here is in the context of researching motor skill and control, including aspects of motor coordination, motor behavior, and motor learning. Thus, performance characterization and assessment of investigator-designed pure pursuit tracking tasks are the focus of the new methodology being presented.

Usually in these motor function tasks the pursuer position is established through some motor action such as movement of a body part or movement of an external object, a cursor on a computer monitor for example, through signal transduction of force generation or other neuromotor activity. Typically, coordinate data for both the target position and the pursuer position are recorded at design-specified intervals as the target progresses along a design-specified path. In deterministic tasks the target position at any given instant is determined *a priori* by the task design. The complexity of experimental designs that have been used is quite broad with target and pursuer trajectories embedded in varying dimensionalities of an original fixed coordinate system and various pursuer position generation mechanisms can be involved. These variations can range from target and pursuer trajectories being embedded in a one-dimensional space[8] to both trajectories being embedded in a three dimensional space, such as that used in robotic rehabilitation[9]. Embedding space dimensionalities for trajectories within a specific pursuit tracking task design are not necessarily uniform. For example, a pursuer trajectory embedded in two-dimensional space generated from coordination of simultaneous force production by two digits of the hand can accompany a target trajectory embedded in one-dimensional space[6], and fingertip force vectors embedded in three-dimensional space can be electronically transduced by force sensors to form a pursuer position trajectory embedded in one dimension on a computer monitor[10].

Some pursuit events may not have the target trajectory under investigator control or not have the pursuer

trajectory involve direct sensor contact. In such cases the position coordinates may require surveillance tracking of pursuer and target coordinates at each sampling instance. This can result in a certain amount of uncertainty or noise in the data since coordinate positions are not specified by the investigator or digitally generated by pursuer contact with recording instrumentation. Multiple detector arrays covering the pursuit event space and new signal processing tools such as those involving finite set theory[11] and collaborative detection frameworks[12] can help optimize accuracy of the original reference frame coordinate values, but subsequently the procedure for defining and obtaining values for target-centric angles is the same as the methodology being presented here.

Objective assessment of a pursuit tracking task performance requires a set of dependent variables derived from position coordinates of the pursuer and the target that can be quantitatively evaluated for each data sampling instance. The fundamental variable, given the nature of pursuit, is the Euclidean displacement distance of the pursuer position from the target position at the moment of each data sampling. This variable has been used ubiquitously over the decades since the pioneering work of Pew[13]. For some tasks in which the target is a large area that can easily be occupied simultaneously by the pursuer the target proximity is sometimes measured as a binary Boolean variable, on or off target, but normally pursuer displacement from the target is a continuous function. Depending on the ultimate information being sought or hypothesis being tested, this fundamental pursuer displacement variable can be viewed as task performer error, as an indirect measure of task performer accuracy, or as an empirical, non-judgmental descriptor of pursuer positioning.

The displacement distance from the pursuer position to the target position is essentially one-dimensional regardless of the vector's orientation with respect to any reference frame and does not convey information concerning the orientation distribution of displacement in higher dimensions. In fact spatial orientation of the pursuer-to-target displacement vector is rarely considered in pursuit tracking evaluation, likely because of ambiguity about what position constitutes an appropriate angle vertex and what reference line is most appropriate for angle magnitude determination in a fixed original reference frame. Another possible reason for this neglect is that the angular orientation of a displacement vector itself is not a direct factor in target proximity computation. Nevertheless, analysis of transient angular information during the course of a pursuit has the potential to provide insight into non-volitional biases such as a confounding tremor contribution[14] and insight into volitional

maneuvering strategies being used by the pursuer, such as response to a visual prompt[15].

Orientation of a distal spatial position with respect to a specific position on a reference line or plane can be described by $v - 1$ independent angles in a v -dimensional system. Presented here is a method for determining those angles together with simplified algorithmic procedures for obtaining their magnitudes using position coordinates obtained at each individual measurement, with the intent that their aggregate statistical properties during a pursuit tracking event can assist in quantitatively characterizing overall performance.

2 Method

2.1 Vertex location for pursuit characterization angles

To define any angle, three points are needed, one of which would become the vertex around which the angle is subtended. Panel (a) of Fig. 1 depicts this construction of a quite simple angle descriptor, ξ , subtended by the displacement pursuer-to-target around the origin of a fixed coordinate-system (or of the laboratory reference-system). It should be clear that because the origin of this system is static, angle ξ will become increasingly restricted in range as the pursuer and target travel away, which renders it use not very well-suited as a descriptor. This can be improved by defining instead a target-centric bearing angle ψ as shown in panel (b) of Fig. 1. Here the vertex has been taken to be the location of the target G . One side of the angle is given by the line joining the instantaneous positions of target and pursuer. The second side of this

angle is provided by the tangent to the target trajectory at its current position G .

The vertex of this example is dynamic rather than static and its position shifts continually as the target traverses its path, thereby accommodating a full range of angle values. For this reason, let us define a local reference frame with the origin at the instantaneous target location G and use the angle ψ as a relevant angle variable to describe the data. There remains, however, the need to transform the data recorded in the laboratory system onto the moving local system. This can be achieved with a combination of translations and rotations of the coordinates recorded in the laboratory system (see Appendix 1).

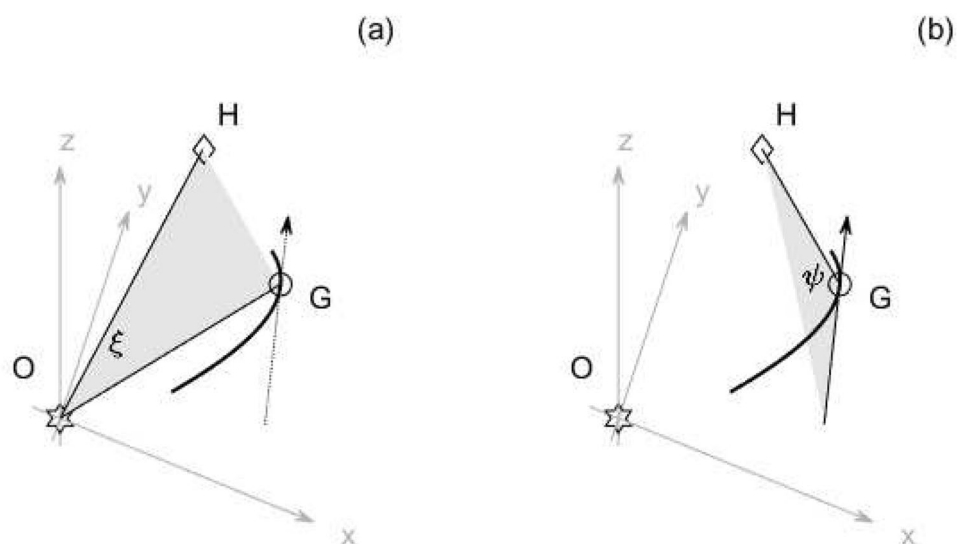
2.2 Conventions for angle rotation and magnitude

Throughout this presentation counterclockwise rotations are described by positive-valued angles, and negative-valued angles indicate clockwise rotation. Angle magnitudes are expressed in radians unless otherwise indicated.

2.3 A consistent local reference frame for individual data samplings

In the general case of a three-dimensional system, each data sampling instance m in a sequence of M will consist of measurements of six variables (three target position coordinates and three pursuer position coordinates), recorded in a generic static reference frame Q_0 which may be arbitrary or may have its axes origin position defined by a particular laboratory or measurement system configuration. Without loss of generality, a right hand Cartesian coordinate system having axes $\{x_0, y_0, z_0\}$ with an origin at $\{0, 0, 0\}$ is assumed to be the original reference

Fig. 1 Diagrams of subtended angles in pure pursuit tracking: **a** the angle ξ between radial vectors to the target position G and to the pursuer position H , having its vertex at the origin O of a static initial reference frame; and **b** the angle ψ whose vertex is at the target position G and having one side formed by the tangent to the target trajectory taken at the target's current position G and the other side formed by a radial vector from the vertex at G to the pursuer position H



frame of data collection. The plane containing the x_0 and y_0 axes constitutes an original reference frame azimuth plane and the z_0 axis is then an initial frame polar axis.

A transient local reference frame is now developed with algorithmic consistency, applicable to each individual data sampling instance, wherein the target's position and current trajectory direction from the perspective of the pursuer position remain constant throughout the pursuit event. This local configuration is one in which the target position defines the local frame origin and in which the tangent line to its current trajectory lies along the x axis pointing in the positive direction. The negative x axis in this local frame then serves as an azimuth directional line such that a pursuing entity directly behind the target on the target's trajectory path has a zero-valued angle of rotation between the target's current trajectory direction and the pursuer's displacement vector from the current target position. If the target trajectory is described by a differentiable curve, then the tangent line to that trajectory can be found at each instantaneous target location and can be used as a reference line to align the x axis of the local reference frame. Any point on that tangent line behind the target can serve as a third position for defining angles with a vertex at the current target position (cf. G in Fig. 1). If a tangent to the trajectory is not available, an approximation to the tangent can be achieved by using a line from the target position at the previous sampling instance to the current target position.

Independently for each sampling instance m the original static reference frame is subjected to seven consecutive rigid body geometric operations (translation along three axes and rotations around four axes) to obtain a geometrically consistent local orientation in

which the target location and trajectory direction are constant from the perspective of the pursuer location. Thus, all positioning data of target and pursuer in the local frame will have a representation independent of the instantaneous direction of the target trajectory, which allows for consistency in defining and interpreting the dynamics of the pursuit behavior.

The reference frame notation used here as the reorientation takes place is of the form $Q_n \{x_n, y_n, z_n\}$ where n is the number of rigid body operations in an explicit sequence that have been applied at that point. Thus, the original orientation of the data from an individual sampling instance, before any geometric maneuvers, is the reference frame Q_0 . For each individual data sampling instance there are three primary positions which are used to specify the configuration for frame Q_n : a position F , located on a trailing tangent line to the target trajectory at the target position, or alternatively the position which had been the location of the target at the immediate prior sampling instance (used to establish the local frame target trajectory direction); the position G , which indicates the current position of the target; and the position H , which indicates the current position of the pursuing entity.

Let the coordinate values of these positions in frame Q_n be denoted as $F(fx_n, fy_n, fz_n)$, $G(gx_n, gy_n, gz_n)$, etc. The process for reference frame reorientation from the original fixed global system Q_0 to a consistent local form Q_7 is fairly straightforward but the details of computation are quite extensive and thus shown separately in Appendix 1. After reorientation to a consistent local frame configuration several position coordinates have a value of zero, namely gx_7, gy_7, gz_7, fy_7 , and fz_7 . In addition $fx_7 < 0$. An illustration of the reorientation of the $\{F, G, H\}$ locations for a random

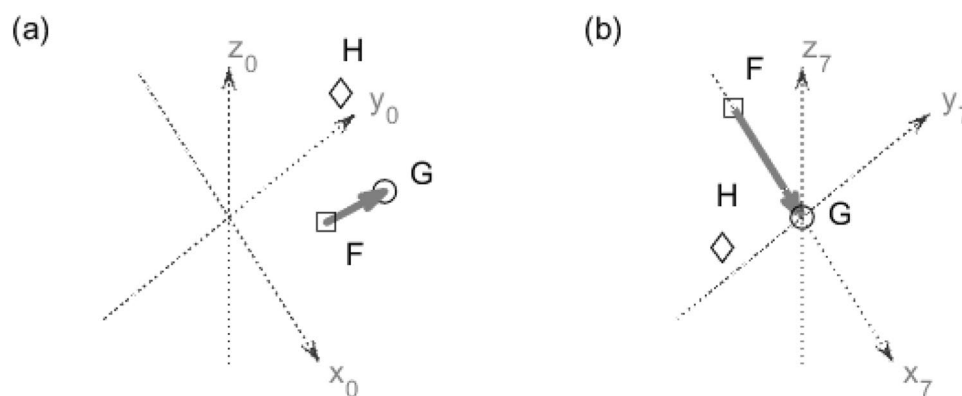


Fig. 2 Reference frame reorientation for a random individual data sampling instance. The positions F (tangent line reference point location), G (current target location), and H (current pursuer location) are indicated with square, circular, and diamond markers, respectively: **a** positions for an initial configuration with axes $\{x_0, y_0, z_0\}$; and **b** configuration after seven consecutive rigid body operations, establishing a new reference frame orientation

with axes $\{x_7, y_7, z_7\}$. The arrow vector from F to G in each panel represents the current target trajectory direction. Note that in panel **b** this vector lies along the negative x_7 axis pointing in the positive direction, and that the current target position G is at the origin. The vector length in both panels is the same though visual perception in the graphic is impacted by the particular spatial observation point used

data sampling instance (sequence number not specified since all samplings are reoriented identically), going from the original static reference frame Q_0 to the local reference frame configuration Q_7 , is shown in Fig. 2 for the case where the final discretionary rotation angle around the x_6 axis to form frame Q_7 is set to zero.

2.4 Characterization angles for pursuit tracking

The positions F , G , and H determine an intrinsic bearing angle with the vertex at G which is independent of reference frame orientation. It is the same as the angle ψ depicted in panel (b) of Fig. 1. There are also other common navigational angles of potential interest in pursuit tracking studies involving the target position G and the pursuer position H whose valuations are dependent on the local reference frame configuration. These angles are determined by another position P specified as the

projection of H on to the local frame's $\{x, y\}$ azimuth plane. The x axis of the final local frame orientation is determined by the target trajectory but generally there is not an orthogonal target attribute available to specify a particular direction for the y axis in that frame. Thus, the reorientation procedure given in Appendix 1 includes a final discretionary rotation about the x_6 axis in frame Q_6 to orient a y_7 axis in a final local frame Q_7 .

The target-centric navigational angles that are of potential interest when the original frame target or pursuer trajectories are embedded in three-dimensional space are then: an azimuth angle θ , formed from F , G , and P ; an elevation angle ϕ , formed from P , G , and H ; and a polar angle ζ , which is merely a right angle complement of ϕ and measures the declination of the pursuer position from the zenith. A graphic representation of these angles, all of which have their vertex at G , is given in Fig. 3.

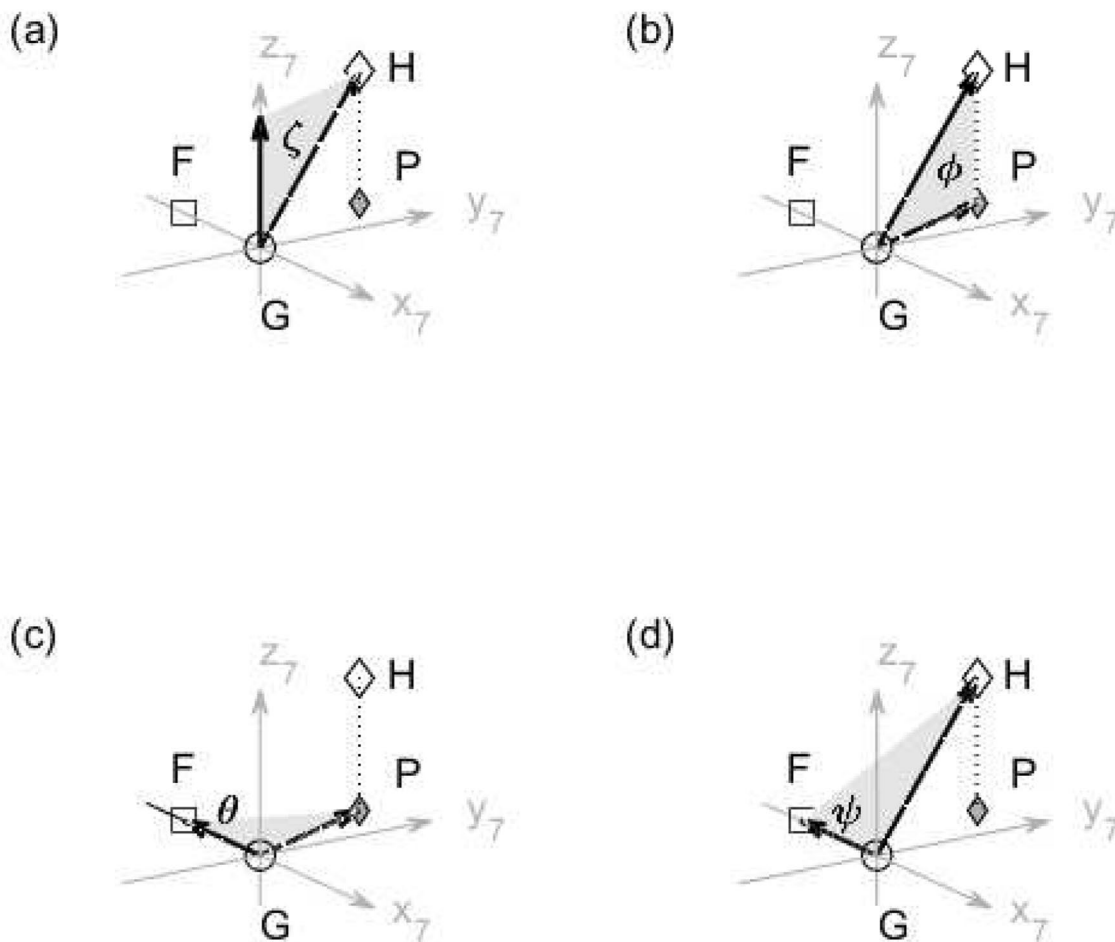


Fig. 3 Pursuit tracking angles in the local frame Q_7 . The two sides of these angles can be described by radial vectors from the current target position G to a pair of other specific local frame positions: **a** the polar angle ζ ; **b** the elevation angle ϕ ; **c** the azimuth angle θ ;

and **d** the bearing angle ψ . In each panel the two vectors forming the angle are displayed as arrows and the subtended angle is shaded

When both the target and pursuer trajectories are embedded in two-dimensional space the pursuer position coincides with its azimuth plane projection position and thus the bearing and azimuth angles are equivalent, i.e., $\psi = \theta$.

2.5 Establishment of a local frame azimuth plane

As is outlined in Appendix 1, six sequential uniform rigid body geometric operations performed on an original reference frame Q_0 will generate a consistent local target-centric reference frame Q_6 having the origin at the target position and the instantaneous target trajectory direction pointing in the positive x_6 axis direction. This is the desired final orientation for the local frame x axis. However, there is still a rotational degree of freedom of the $\{y_6, z_6\}$ plane around the x_6 axis and such a rotation by an investigator-specified angle α^* is needed to obtain a final unambiguous local reference frame Q_7 where the $\{x_7, y_7\}$ plane is the final local frame azimuth plane. The mechanics for carrying out this final geometric operation are outlined in Appendix 1. The simplest choice for α^* is $\alpha^* = 0$, in which case local reference frame Q_7 is identical to frame Q_6 . In this instance the local frame azimuth plane is predetermined solely by the orientation of the initial reference frame Q_0 , which itself may have been specified such that a certain axis aligns parallel or perpendicular to some external field or gradient. This choice of zero rotation around the x_6 axis can be considered as a default for determining the local frame azimuth plane, and should be satisfactory as long as the physical environment around the target is isotropic during the pursuit event. Another convenient choice for α^* , if only the bearing angle ψ is of interest, is setting it equal to the arctangent of the ratio of the negative of the pursuer z coordinate value in Q_6 to the pursuer y coordinate value in Q_6 . In this instance the pursuer z coordinate value in Q_7 always evaluates to the constant zero and thus the pursuer location is always in the local frame azimuth plane, thereby reducing the system to two-dimensional. Other less general choices for α^* may be made derived indirectly from the measured coordinate values of the pursuer position in the original frame Q_0 . As an example, an investigator may want the largest possible range of elevation angle ϕ magnitude values to be present in local frame Q_7 . Plots of ϕ as a function of sampling number over the course of the pursuit for differing test values of α^* could help to identify an optimum value of this angle for maximizing the range of ϕ .

2.6 Determination of angle values from position coordinates

All computational procedures were done using MATLAB®. The cosines of the angle variables were determined using position coordinates in the local reference frame Q_7 and the law of cosines. Because of the trigonometric relationship $\cos(-\omega) = \cos(\omega)$ and the periodic relationship $\cos(\omega) = \cos(\omega \pm 2k\pi)$ for any integer k , angles cannot be determined simply by using their cosines as arguments for the arccos function. Here we restrict angles to be single-valued in the interval $(-\pi, \pi]$. This process is greatly simplified in the local reference frame, though the values of the angles themselves will be the same as if they had been determined using original reference frame coordinates of system positions. Even with a simplified process, however, the computations are still somewhat involved. Thus, the details are shown separately in Appendix 2.

2.7 Procedures for obtaining example experimental data

To illustrate application of angles as variables in pursuit tracking characterization, the bearing angle ψ has been calculated for samplings from an example experimental data set. Pursuer and moving target coordinate data were collected in a time series with a sampling rate of 200 Hz during the course of a particular tracking task performance. The task design, based on that of Lewis[16], consists of a performer-controlled cursor (the pursuing entity) tracking a target ball that is moving along a square diamond path being displayed on a flat vertical computer monitor screen. Data acquisition instrumentation employed in producing force-related position vectors used in this example has been described in detail by Spirduso et al.[17]. The cursor position on the monitor screen is moved by simultaneous application or lessening of force on two identical stationary force sensors. The horizontal cursor position is determined by the force level applied to one sensor with the right hand thumb and the vertical cursor position is determined by the force level applied to the other sensor with the right hand index finger in a precision pinch grip. Increasing thumb force moves the cursor to the right and increasing finger force moves the cursor upward. The system is two-dimensional with the original reference frame Q_0 having its $\{x_0, y_0\}$ origin at the location where the cursor is situated when no force is exerted on either sensor. Distances are dimensionless and scaled to the task performer's maximum voluntary contraction force (MVC) for each respective digit. The

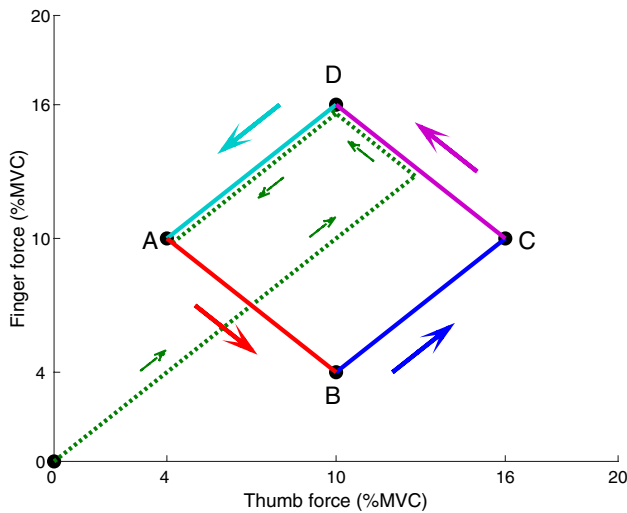


Fig. 4 Task target ball trajectory in the original reference frame Q_0 . After preliminary maneuvering to reach the analysis region starting point A (dotted path), the target moves counterclockwise along segments that represent four types of digit force modulation patterns: segment AB (corresponding to increasing thumb force, decreasing finger force); segment BC (corresponding to increasing force by both digits); segment CD (corresponding to decreasing thumb force, increasing finger force); and segment DA (corresponding to decreasing force by both digits). Each segment represents a change magnitude of 6% MVC for each digit and the target moves from segment start to segment end in 3 s, comprising about 600 samplings per segment

target ball pathway is controlled by custom LabVIEW® software and is illustrated in Fig. 4.

The experimental data presented here for illustration comes from a single task trial performed by an 18 year old, right-handed male volunteer participant. A task administration protocol approved by the local Institutional Review Board was used. Instructions were to try keeping the cursor as close as possible to the position of the moving target ball by modulating digit forces, but without mention of any preferred angular orientation with respect to the target trajectory.

3 Results

3.1 Angles as functions of the local frame pursuer position

Using the methodology shown in Appendix 1 positions in the original reference frame Q_0 were transformed to the equivalent positions in the local reference frame Q_7 . The expressions for angle variables of interest derived in Appendix 2 Equations (21), (22), and (23) are then able

to be stated in terms of the pursuer position coordinates $\{hx_7, hy_7, hz_7\}$ exclusively:

$$\phi = \left(\frac{hz_7}{||hz_7||} \right) \left| \arccos \left(\frac{\sqrt{hx_7^2 + hy_7^2}}{\sqrt{hx_7^2 + hy_7^2 + hz_7^2}} \right) \right|. \tag{1}$$

$$\theta = - \frac{hy_7}{||hy_7||} \left| \arccos \left(\frac{-hx_7}{\sqrt{hx_7^2 + hy_7^2}} \right) \right| \tag{2}$$

$$\psi = - \frac{hy_7}{||hy_7||} \left| \arccos \left(\frac{-hx_7}{\sqrt{hx_7^2 + hy_7^2 + hz_7^2}} \right) \right|. \tag{3}$$

Although these angle variable values are independent of reference frame orientation when all reorientation is with rigid body maneuvers, they are not independent of each other. Furthermore, as derived in Appendix 2 and shown in Eq. (20), ψ can be formed implicitly as a function of ϕ and θ , i.e., $\cos \psi = \cos \phi \cos \theta$.

3.2 Valuation of angles in special cases

In addition to the general case where none of the local frame pursuer position coordinates $hx_7, hy_7,$ and hz_7 have value zero, there are seven other situations where one or more of those coordinates do have value zero: three where exactly one of them has value zero, three where exactly two of them have value zero, and a single case where all three of them have value zero, i.e., the pursuer position coincides exactly with the target position.

Considering limits for $hy_7 \pm \epsilon$ and $hz_7 \pm \epsilon$ as $\epsilon \rightarrow 0$ we will use the conventions that $\frac{hy_7}{||hy_7||} = 1$ when $hy_7 = 0$ and that $\frac{hz_7}{||hz_7||} = 1$ when $hz_7 = 0$. Furthermore, we will use the conventions that $\phi = \theta = \psi = 0$ when the pursuer position is exactly at the target position. Using these conventions to modify where necessary in the special cases, the modified general Eq.s (1), (2), and (3) can provide valuations for all the pursuit tracking angle variables of interest in all cases.

The special case where the target trajectory and the pursuer position are confined to a two dimensional plane, for example a performer-controlled cursor following a moving target position on a flat computer monitor screen, will have all the local frame positions in an $\{x_7, y_7\}$ azimuth plane with $fx_7 = gx_7 = hz_7 \equiv 0$ for every data sampling instance. Thus, the pursuer position H coincides with

its projection P on the azimuth plane and hence Eq. (3) collapses to the form of Eq. (2) such that $\psi = \theta$.

3.3 Example angle usage with experimental data

The experimental data set which is being used here for illustrating the usage of an angle as a descriptive variable belongs to one of the special cases, a two-dimensional configuration in which all positions have z coordinate values at zero so that both target and pursuer trajectories lie in an $\{x, y\}$ azimuth plane, thus having $\phi \equiv 0$, and $\psi = \theta$. Thus, there is only one degree of rotational freedom for an angle descriptor so that analysis can be comprehensively conducted by evaluating only the bearing angle ψ . When the original reference frame is transformed to the local reference frame Q_7 for all samplings, the position of the pursuing cursor can be assigned to one of four quadrants

of the $\{x_7, y_7\}$ azimuth plane. These quadrants are defined as follows: Quad I is bounded by the negative x_7 axis and negative y_7 axis and represents cursor positions where ψ would be an acute counterclockwise rotation angle from the azimuth reference line; Quad II is bounded by the positive x_7 axis and negative y_7 axis and represents cursor positions where ψ would be an obtuse counterclockwise rotation angle; Quad III is bounded by the positive x_7 axis and positive y_7 axis and represents cursor positions where ψ would be an obtuse clockwise rotation angle; and Quad IV is bounded by the positive y_7 axis and negative x_7 axis and represents cursor positions where ψ would be an acute clockwise rotation angle.

In the example task, which has a counterclockwise target trajectory circuit in the original Q_0 reference frame as shown in Fig. 4, a cursor position in Quad I corresponds to it being behind the target on the exterior side of the circuit with $0 \leq \psi < \frac{\pi}{2}$; a cursor position in Quad II

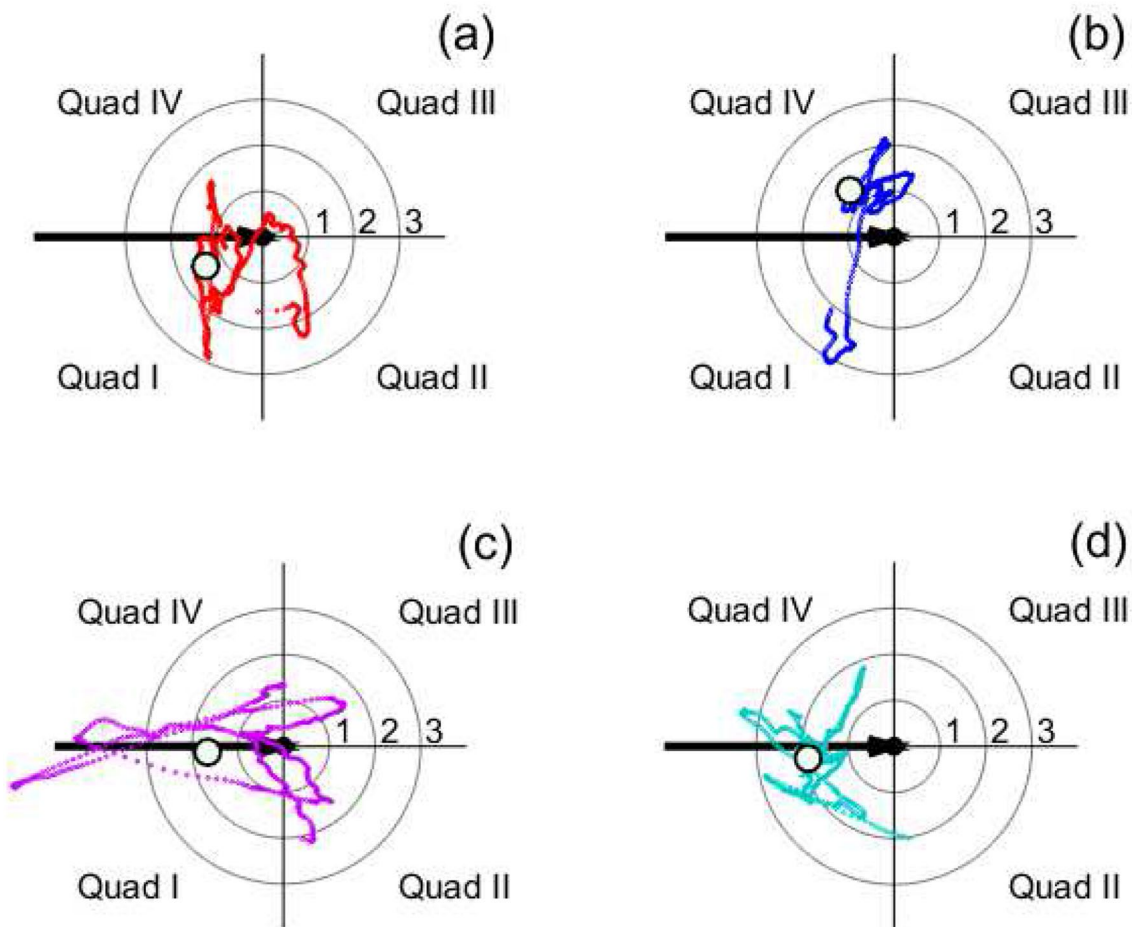


Fig. 5 Local frame Q_7 scatter plots of cursor coordinate pairs $\{x_7, y_7\}$ for samplings taken during each of four target trajectory segments as shown in Fig. 4: **a** segment AB (increasing thumb force, decreasing finger force); **b** segment BC (increasing thumb force, increasing finger force); **c** segment CD (decreasing thumb force,

increasing finger force); and **d** segment DA (decreasing thumb force, decreasing finger force). The circular lines are contours of constant distance of the cursor from the target in % MVC units and the larger dot in each panel indicates the mean cursor $\{x_7, y_7\}$ position during pursuit in each segment

corresponds to it being ahead of the target on the exterior side of the circuit with $\frac{\pi}{2} \leq \psi < \pi$; a cursor position in Quad III corresponds to it being ahead of the target on the interior side of the circuit with $-\pi < \psi \leq -\frac{\pi}{2}$; and a cursor position in Quad IV corresponds to it being behind the target on the interior side of the circuit with $-\frac{\pi}{2} < \psi \leq 0$.

This quadrant division of cursor positions for the example task performance is shown in Fig. 5 using separate panels for data in each individual task segment. The $\{x_7, y_7\}$ positions of all samplings during each of the four target trajectory segments (AB, BC, CD, and DA as defined in the original frame Q_0) are displayed as small dots in scatter plots. There is a larger dot in each scatter plot panel indicating the mean cursor position in the local reference frame Q_7 for the respective segment.

It can be inferred from this Fig. that in the original reference frame the mean position of the cursor was behind the target on the exterior side of the circuit for all segments except BC, where both digit forces were increasing. In that exceptional case the mean position of the cursor was behind the target as well but on the

interior side of the circuit. Segment BC also had the largest magnitude for the mean value of ψ .

Patterns of fluctuation in the value of the bearing angle ψ in sequential data samplings as the target traversed the four segments of its path are displayed in Fig. 6. The fluctuations of ψ within the various segment regions, seen in panel (a) of this figure, do not seem to have any regularity in their temporal patterns. When considering the fluctuation of the absolute value of the magnitude of the angle ψ around its mean, depicted in panel (b) of the figure, it is seen that the variation is much greater within

Table 1 Mean values of variables (with standard deviations) by target trajectory segment

| Segment | ψ (°) | $ \psi $ (°) | cursor displacement from target (% MVC) |
|---------|-----------------|-----------------|---|
| AB | 27.0° (±74.2°) | 64.6° (±45.43°) | 1.4 (±0.6) |
| BC | -46.6° (±52.9°) | 68.1° (±18.1°) | 1.4 (±0.6) |
| CD | 4.4° (±79.2°) | 60.9° (±50.8°) | 1.7 (±1.4) |
| DA | 8.1° (±27.9°) | 22.5° (±18.5°) | 1.9 (±0.5) |

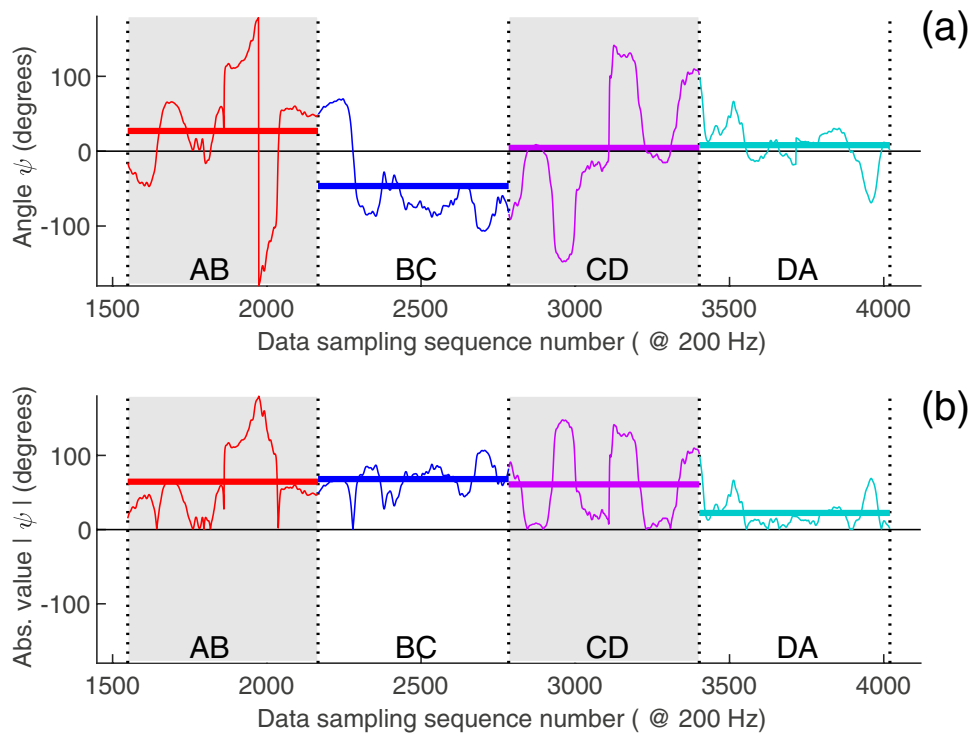
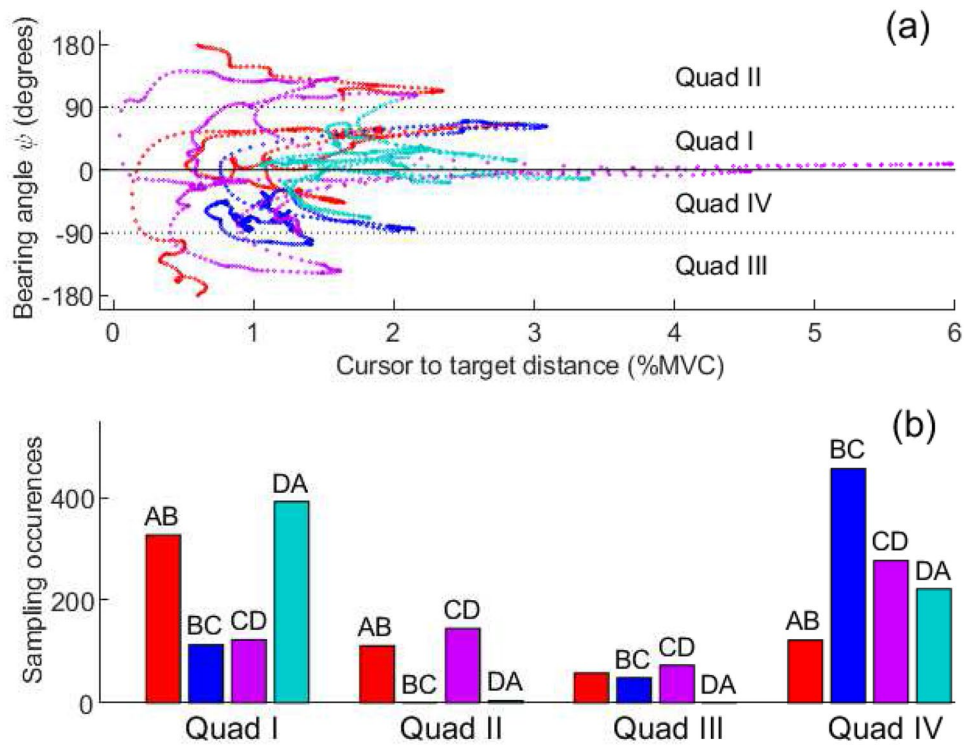


Fig. 6 Fluctuations in rotation of the bearing angle ψ (displayed in terms of circular arc degrees rather than in radians for conceptual convenience) over the four target pathway segments in the example pursuit tracking task performance: **a** true signed angle values as a function of task progress and **b** absolute angle values as a function of task progress. The horizontal bars indicate the mean value over data samplings within a particular segment.

Segments where the force modulation requirements (increasing or decreasing force application) are opposite for the two digits controlling the cursor position appear with a shaded background. Sampling number values reflect sequential sampling ordering, which takes into account sampling instances recorded during the preliminary maneuvers getting the target to the starting position of segment AB

Fig. 7 Geometric distribution of individual data sampling ψ values by their associated Q_7 frame quadrants over the four segments for the example task performance: **a** scatter plot of ψ values versus cursor proximity to the target and **b** histogram of ψ value occurrences for the four segments aggregated by their associated Q_7 frame quadrant bins



segments where the force modulation requirements for the two digits are in opposite directions (segments *AB* and *CD*) than it is where the force modulation requirements by the two digits are in the same direction (segments *BC* and *DA*). The numerical mean values and standard deviations of ψ over all four task segments for the example task performance are shown in Table 1.

A scatter plot of the bearing angle ψ versus the distance of the cursor from the target in all four task segments collectively is shown for this particular performance in panel (a) of Fig. 7. From the display in this panel there does not appear to be any discernible simple functional relationship or correlation of the value of ψ with target proximity of the cursor. However, if occurrences of ψ values are aggregated by associated quadrants into a histogram, as shown in panel (b) of the figure, certain phenomena become apparent. Foremost, the cursor stays behind the target (Quad I and Quad IV) most of the time in all segments and almost exclusively during target traversal of segment *DA*. Also, the cursor gets ahead of the target (Quad II and Quad III) with greater frequency within segments where the force modulation requirements for the two digits are in opposite directions (*AB* and *CD*) than it does within segments where they are in the same direction (*BC* and *DA*). Furthermore, the cursor position is more often on the exterior side of the target circuit (Quad I and Quad II) in segments where the modulated finger force is decreasing (*AB* and *DA*) and more often on the

interior side (Quad III and Quad IV) in segments where the modulated thumb force is increasing (*BC* and *CD*).

4 Discussion

4.1 Choices for characterization angles and local reference frame

Any three distinct spatial points and linear lines connecting them are sufficient for defining an angle with a vertex at one of the points. If two of the three points include a pursuing entity position and a target position themselves or directly related points (such as projections on to specific axes or planes), then the angle formed is descriptive in some sense of the pursuit event at each particular data sampling instance. With the reference position being arbitrary there are an unlimited number of such descriptive angles possible, but here we have chosen a reference point that can be used in describing the current target trajectory direction or the direction from the target to the projection of the pursuer position on to the azimuth plane. The choice of using the current target position as the vertex for all the descriptive angles being considered here assures that the range of their magnitudes is not impacted by the remoteness of the target from the origin in the static original reference frame. The local reference frame orientation is chosen such that pursuer positioning with respect to the target trajectory

direction remains the same for all data sampling instances, providing a sense of being above, below, ahead, behind, to the left, or to the right of the target in terms of its current trajectory direction. This permits the distribution of displacement orientation information from individual data samplings based on assignment to specific spatial regions surrounding the current target position.

Furthermore, the consistent local frame orientation that has been chosen accommodates a simplified procedure for obtaining the cosines of all the characterization angles. Although nine position coordinates are needed for reorienting the original reference frame (those of the pursuer, target and reference point locations), only three local frame coordinate positions (those of the pursuer location) are required for computing the cosines of those angles.

Selecting the target trajectory direction to be the local frame x_7 axis is a bit arbitrary but it is convenient since typical geometric nomenclature designates x as a first Cartesian axis in systems of any dimensionality.

4.2 Interpretation of angle variables

In most cases the overall goal in a pursuit tracking task is for the pursuer position to match that of the target as closely as possible for the duration of the pursuit event. Therefore, the displacement distance of the pursuer position from the target position at each data sampling instance is normally used as an indicator of performance error or accuracy without consideration of the spatial orientation of that separation. The orientation itself is not directly a computational factor in obtaining the magnitude of the displacement so it is commonly disregarded, but the characterization angles defined here can be interesting auxiliary descriptors in multidimensional systems. In the context of the local reference frame the elevation angle indicates whether the pursuer position is above or below the azimuth plane. The azimuth and bearing angles both indicate a lateral positioning (left or right side) of the pursuer position with respect to the target trajectory direction. Furthermore, the bearing angle indicates a longitudinal positioning (behind or ahead) of the pursuer position with respect to the target position. In addition to the positioning indications the azimuth and bearing angles also establish the pursuer position within specific local frame spatial regions surrounding the target position (quadrants in two dimensions or octants in three dimensions). These characterization angles may not matter in some situations, particularly linear systems where they are constants or have trivial variability. However, in multidimensional systems the values of these angles can be of importance for those tasks in which a specific preferred orientation for displacement, such as staying

directly behind the target on its trajectory path, is included in the intended performance objective of the task design.

The characterization angles are dynamic and though their magnitudes are independent of reference frame orientation, they are time-dependent and can vary from sampling to sampling. A pursuit task performance thus needs to be assessed in the context of statistical properties and distributions of angle valuations over all data samplings recorded. If there are a sufficient number of samplings and the mean values of the angles are not near zero, then there may be systematic orientation biases that could be investigated. Also, because the ranges of possible values for the characterization angles are symmetric around zero, the variances around the means and the means of their absolute values can also be informative.

Like any other dependent variable, the characterization angles and their statistical within-task attributes can be used for inferential characterization of aggregate performance in a hierarchical structure of sampling within task trial within specific pursuer entity within group, etc. For the pursuer-target displacement distance variable it is common to use its standard deviation from the mean (*RMSE*) as an aggregate attribute, though the mean absolute error (*MAE*) has been suggested as a better alternative[18]. Analogous aggregate orientation attributes of displacement vectors can likewise be specified using distributions of the characterization angle values, as has been illustrated in Table 1 for the bearing angle.

4.3 Characterization of the example pursuit tracking task performance

The bearing angle evaluations from the example data set presented here in Sect. 3.3 illustrate various ways in which this dependent variable can play a part in characterizing a multidimensional pursuit tracking event. A pursuit tracking task of this particular design was specifically chosen because performance involves usage of multiple motor skills and because the task difficulty is substantial enough that the bearing angle variable takes on a wide range of values during the pursuit. The natural tendency in generating forces in a two digit pinch grip, as is the case in this example, is to exert equal force levels with modulation (increasing or decreasing) in the same direction for the two digits, but in this task each of the four segments requires a differing pattern of modulation over differing force ranges for the digits. Thus, both fine motor control skill and motor coordination skill are involved. Also, the displacement orientation fluctuations shown in panel (a) of Fig. 6 confirms that fluctuation of bearing angle values occur over a very large fraction of the possible

360° rotation range from the local frame target trajectory reference line.

This particular task performance example is intended merely to illustrate the mechanics of obtaining angle values and to show potential uses of the variable ψ , the bearing angle. A few features of the particular trial presented here, detailed in Sect. 3, are apparent. For example, the distribution of values for the bearing angle ψ over all data samplings during the task performance is not uniform or completely random, but instead is concentrated behind the target in quadrants I and IV of the local reference frame.

4.4 Limitations

The mechanics of reorientation of an original static frame to a local reference frame for an individual data sampling event and the subsequent computation of the elevation, azimuth, and bearing angles for the pursuer position are straight-forward using the methodology presented in Appendices 1 and 2. However, the target cannot remain stationary with respect to the original reference frame Q_0 from one sampling instance to the next. Otherwise the task becomes a matching task rather than a pursuit task. Also, there can be ambiguity in angle definition and computation if the pursuer position coincides with the target position exactly for a sampling instance, resulting in a zero distance vector for the displacement of pursuer position from the target position. Another important caveat, if the target position of the immediate prior data sampling instance is being used as a proxy for a tangent line reference point F , is that data sampling must be frequent enough such that a vector from F to the current target location G captures an adequate approximation of the direction of the target trajectory in the local frame. Other problems may arise if the target trajectory in the original Q_0 reference frame is frequently changing its direction abruptly or in substantial ways such as in Brownian motion or in a random walk.

5 Conclusion

Angle variables describing pursuer positions during pursuit tracking with respect to the current direction of the target trajectory can give a more localized perspective of pursuer performance than can angle variables describing positional relationships to a fixed point, such as the origin of a static global reference frame. Using rigid body geometric translation and rotation operations, each sampling of positional data can be transformed such that the target is at the origin of a new local frame and

its trajectory is along the x axis in that new frame, with the negative x axis direction serving as a reference line for angle construction. This allows establishment of a bearing angle variable ψ that can be used to classify the pursuer position in terms of quadrant spatial regions around the target for a two-dimensional system. The distribution and dynamics of angle variables related to the pursuer location within a local frame traveling with the target can potentially give insights about behavioral characteristics as well as systematic biases of the pursuer performance during pursuit.

Acknowledgements The author is grateful to L. Abraham for helpful discussion and commentary concerning the need for and usefulness of angle variables in pursuit tracking studies and to anonymous reviewers of this work who provided numerous suggestions that contributed greatly to enhancing its clarity, precision, and brevity. Thanks are also extended to M. Schleicher for kindly providing the example data set along with granting permission for its usage in constructing illustrative figures. The help of H. Karamchandani in administering the particular task protocol used for the experimental example is appreciated, as is the contribution of an anonymous volunteer participant who generated the example data set by performing the task.

Compliance with ethical standards

Conflict of interest The author states that the content of this work presents no conflict of interest.

Appendices

1. Coordinate frame reorientation

The process of reorienting an initial static global reference frame Q_0 to a consistent local configuration Q_7 using initial frame pursuit tracking coordinate data for the current pursuer and tracking positions is quite extensive but can be accomplished with ordinary matrix algebra techniques associated with rigid body maneuvers. The final orientation is dependent on the current target trajectory direction, which requires coordinates of a reference position F in addition to the coordinates of the pursuer position H and target position G . Position F can be any point behind the moving target position on a line tangent to the target trajectory at its current location if such is available, or with rapid enough coordinate data sampling, an approximate tangent line location can be made by using the location of the target at the immediate prior sampling instance.

First, the initial coordinate position values of F , G , and H for the sampling are assembled into a 3×3 column vector matrix \mathbf{M}_0 :

$$M_0 = \begin{pmatrix} fx_0 & gx_0 & hx_0 \\ fy_0 & gy_0 & hy_0 \\ fz_0 & gz_0 & hz_0 \end{pmatrix}. \tag{4}$$

The objective is then to transform the reference frame orientation through an explicit sequence of translations along and Euler angle rotations about current frame axes to obtain a final configuration Q_7 in which the current target position is at the origin, its current trajectory direction lies along the negative x_7 axis pointing in the positive x_7 axis direction, and an orthogonal y_7 axis direction is specified to establish a definitive local frame azimuth plane having the negative x_7 axis as the reference line.

Each rigid body maneuver in this process can be represented as a left matrix multiplication of matrix M_{n-1} by a translation or rotation operator O_n in order to form a new matrix M_n , i.e., $M_n = O_n M_{n-1}$. Three of the transformation matrix operators translate the frame along the current x , y , and z axes to put the target position at the origin. The three translation operators are commutative and produce the same outcome regardless of the order in which they are applied. Therefore the aggregate of these translation operations can be obtained in an equivalent matrix representation by subtracting gx_0 from each position's x_0 coordinate value, gy_0 from each position's y_0 coordinate value, and gz_0 from each position's z_0 coordinate value in M_0 . Thus,

$$M_3 = \begin{pmatrix} (fx_0 - gx_0) & (gx_0 - gx_0) & (hx_0 - gx_0) \\ (fy_0 - gy_0) & (gy_0 - gy_0) & (hy_0 - gy_0) \\ (fz_0 - gz_0) & (gz_0 - gz_0) & (hz_0 - gz_0) \end{pmatrix} \tag{5}$$

$$= \begin{pmatrix} fx_3 & 0 & hx_3 \\ fy_3 & 0 & hy_3 \\ fz_3 & 0 & hz_3 \end{pmatrix}.$$

Now G is fixed at the origin for all subsequent coordinate frame rotations based on current frame positions of F and H . The $\{x_3, y_3\}$ azimuth plane contains the target position G and a position P representing the projection of H on to the azimuth plane. Further rigid body operations involve rotations about current axes at G .

Three rotational operators from classical mechanics are then used, (R_x , R_y , and R_z), which rotate the frame counterclockwise: by angle α around the current x axis, by angle β around the current y axis, and by angle γ around the current z axis, respectively.

$$R_x = \begin{pmatrix} 1 & 0 & 0 \\ 0 & \cos \alpha & -\sin \alpha \\ 0 & \sin \alpha & \cos \alpha \end{pmatrix} \quad R_y = \begin{pmatrix} \cos \beta & 0 & \sin \beta \\ 0 & 1 & 0 \\ -\sin \beta & 0 & \cos \beta \end{pmatrix}$$

$$R_z = \begin{pmatrix} \cos \gamma & -\sin \gamma & 0 \\ \sin \gamma & \cos \gamma & 0 \\ 0 & 0 & 1 \end{pmatrix}.$$

The first rotation, around the x_3 axis by an angle α , creates a new matrix M_4 and is accomplished by left matrix multiplication of M_3 by R_x . By choosing α such that $fy_3 \sin \alpha = -fz_3 \cos \alpha$, i.e., $\alpha = \arctan\left(-\frac{fz_3}{fy_3}\right)$, we get the coordinate frame Q_4 with M_4 having the fz_4 element be zero. Therefore, the tangent line reference position F in the new coordinate frame lies in the azimuth plane defined by the new x_4 and y_4 axes:

$$M_4 = R_x M_3$$

$$= \begin{pmatrix} 1 & 0 & 0 \\ 0 & \cos \alpha & -\sin \alpha \\ 0 & \sin \alpha & \cos \alpha \end{pmatrix} \begin{pmatrix} fx_3 & 0 & hx_3 \\ fy_3 & 0 & hy_3 \\ fz_3 & 0 & hz_3 \end{pmatrix}$$

$$= \begin{pmatrix} fx_3 & 0 & hx_3 \\ (fy_3 \cos \alpha - fz_3 \sin \alpha) & 0 & (hy_3 \cos \alpha - hz_3 \sin \alpha) \\ (fy_3 \sin \alpha + fz_3 \cos \alpha) & 0 & (hy_3 \sin \alpha + hz_3 \cos \alpha) \end{pmatrix} \tag{6}$$

$$= \begin{pmatrix} fx_4 & 0 & hx_4 \\ fy_4 & 0 & hy_4 \\ 0 & 0 & hz_4 \end{pmatrix}.$$

Continuing, the next step is to create another new coordinate frame Q_5 by rotation of the current frame Q_4 around the z_4 axis by an angle γ , thus giving a new system position matrix M_5 . This can be accomplished by left matrix multiplication of M_4 by R_z . The objective here is to bring the tangent line reference position F on to the x axis of the new frame, i.e., on to x_5 . By choosing γ such that $fx_4 \sin \gamma = -fy_4 \cos \gamma$, i.e., $\gamma = \arctan\left(\frac{-fy_4}{fx_4}\right)$, we get a new coordinate frame Q_5 with matrix M_5 having the fy_5 element be zero. Thus, the tangent line reference position F in Q_5 has coordinates $\{fx_5, 0, 0\}$ and hence lies on the x_5 axis in the new frame:

$$M_5 = R_z M_4$$

$$= \begin{pmatrix} \cos \gamma & -\sin \gamma & 0 \\ \sin \gamma & \cos \gamma & 0 \\ 0 & 0 & 1 \end{pmatrix} \begin{pmatrix} fx_4 & 0 & hx_4 \\ fy_4 & 0 & hy_4 \\ 0 & 0 & hz_4 \end{pmatrix}$$

$$= \begin{pmatrix} (fx_4 \cos \gamma - fy_4 \sin \gamma) & 0 & (hx_4 \cos \gamma - hy_4 \sin \gamma) \\ (-fx_4 \sin \gamma + fy_4 \cos \gamma) & 0 & (-hx_4 \sin \gamma + hy_4 \cos \gamma) \\ 0 & 0 & hz_4 \end{pmatrix}$$

$$= \begin{pmatrix} fx_5 & 0 & hx_5 \\ 0 & 0 & hy_5 \\ 0 & 0 & hz_5 \end{pmatrix}.$$

(7)

At this stage the target position G is at the origin and a vector from F to G , indicating the target trajectory direction, lies on the x_5 axis. However, it has not yet been established that such a trajectory will always point in the positive x axis direction, i.e., $fx_5 < gx_5 = 0$, so that fx_5 is negative. This problem can be resolved, however, with a rotation around the y_5 axis by an angle β , accomplished by left multiplication of \mathbf{M}_5 by \mathbf{R}_y , thus creating a reference frame Q_6 with a corresponding system matrix \mathbf{M}_6

$$\begin{aligned} \mathbf{M}_6 &= \mathbf{R}_y \mathbf{M}_5 \\ &= \begin{pmatrix} \cos \beta & 0 & \sin \beta \\ 0 & 1 & 0 \\ -\sin \beta & 0 & \cos \beta \end{pmatrix} \begin{pmatrix} fx_5 & 0 & hx_5 \\ 0 & 0 & hy_5 \\ 0 & 0 & hz_5 \end{pmatrix} \\ &= \begin{pmatrix} fx_5 \cos \beta & 0 & (hx_5 \cos \beta + hz_5 \sin \beta) \\ 0 & 0 & hy_5 \\ -fx_5 \sin \beta & 0 & (-hx_5 \sin \beta + hz_5 \cos \beta) \end{pmatrix}. \end{aligned} \tag{8}$$

To keep F on the new x_6 axis we need to have $fx_6 = -fx_5 \sin \beta = 0$, and thus we must choose $\beta = 0$ or $\beta = \pi$. Since $fx_6 = fx_5 \cos \beta$ and since we want this quantity to be negative, the signs of fx_5 and $\cos \beta$ must be opposite, i.e., $\beta = 0$ if $fx_5 < 0$ and $\beta = \pi$ if $fx_5 > 0$. Therefore, our choice for β is

$$\beta = \frac{\pi}{2} \left(1 + \frac{fx_5}{||fx_5||} \right) \tag{9}$$

which has this property, thus reducing Eq. (8) to

$$\begin{aligned} \mathbf{M}_6 &= \begin{pmatrix} fx_6 & 0 & hx_6 \\ 0 & 0 & hy_6 \\ fz_6 & 0 & hz_6 \end{pmatrix} \\ &= \begin{pmatrix} fx_6 & 0 & hx_6 \\ 0 & 0 & hy_6 \\ 0 & 0 & hz_6 \end{pmatrix}. \end{aligned} \tag{10}$$

The reference frame orientation Q_6 then has a configuration where the current target position G is at the origin, the tangent line reference position F is on the negative x_6 axis, and the target trajectory points in the direction of the positive x_6 axis. This is a default local frame having the desired target location and trajectory direction attributes and an azimuth plane specified by the configuration of the original static frame Q_0 . However, a further rotation of this frame around the x_6 axis can adjust the azimuth plane to a preferred orientation without impacting the target attributes. Hence as a final operation the Q_6 frame is rotated counterclockwise around the x_6 axis by an angle α^* (which can be 0 to retain the default azimuth plane orientation), thereby forming a final local frame Q_7 in which a particular direction for the y_7 axis is specified. This creates a new matrix \mathbf{M}_7 and is

accomplished by left matrix multiplication of \mathbf{M}_6 by \mathbf{R}_x having Euler angle α^* :

$$\begin{aligned} \mathbf{M}_7 &= \mathbf{R}_x \mathbf{M}_6 \\ &= \begin{pmatrix} 1 & 0 & 0 \\ 0 & \cos \alpha^* & -\sin \alpha^* \\ 0 & \sin \alpha^* & \cos \alpha^* \end{pmatrix} \begin{pmatrix} fx_6 & 0 & hx_6 \\ 0 & 0 & hy_6 \\ 0 & 0 & hz_6 \end{pmatrix} \\ &= \begin{pmatrix} fx_6 & 0 & hx_6 \\ 0 & 0 & (hy_6 \cos \alpha^* - hz_6 \sin \alpha^*) \\ 0 & 0 & (hy_6 \sin \alpha^* + hz_6 \cos \alpha^*) \end{pmatrix} \\ &= \begin{pmatrix} fx_7 & 0 & hx_7 \\ 0 & 0 & hy_7 \\ 0 & 0 & hz_7 \end{pmatrix}. \end{aligned} \tag{11}$$

The resulting frame Q_7 thus has a specific y_7 axis direction and $\{x_7, y_7\}$ azimuth plane defined. This frame will be used for the configuration of the local reference frame of an individual data sampling instance and corresponds to the coordinate frame diagram shown in panel (b) of Fig. 2. Note that choosing α^* such that $hy_6 \sin \alpha^* = -hz_6 \cos \alpha^*$, i.e., $\alpha^* = \arctan\left(\frac{-hz_6}{hy_6}\right)$, results in hz_7 evaluating as the constant 0 and hence the pursuer and target positions and the dynamics of trajectories occur exclusively in an $\{x_7, y_7\}$ azimuth plane.

2. Obtaining angles in the local frame

To evaluate a particular angle in the local reference frame Q_7 whose vertex is at the origin, where the current target position is located, we use the coordinates of the two positions serving as radial vector terminals for that angle and the lengths of those two associated radial vectors.

For a pair of vectors \mathbf{u} and \mathbf{v} forming an angle at their point of intersection the law of cosines states

$$\cos(\mathbf{u}, \mathbf{v}) = \frac{\mathbf{u} \cdot \mathbf{v}}{||\mathbf{u}|| ||\mathbf{v}||} \tag{12}$$

which is used to determine the cosine values of angles. The inner product in the numerator is the sum $u(x)v(x) + u(y)v(y) + u(z)v(z)$ and the norms in the denominator are of the form $\sqrt{u(x)^2 + u(y)^2 + u(z)^2}$. We note that if the pursuer position H is projected on to the azimuth plane at location P , then the coordinates of P can be expressed as $\{px_7, py_7, pz_7\} = \{hx_7, hy_7, 0\}$. From this we can determine radial vector lengths from the origin to the pursuer position H and to its azimuth plane projection position P :

$$r_7 = \sqrt{hx_7^2 + hy_7^2 + hz_7^2} \tag{13}$$

$$q_7 = \sqrt{px_7^2 + py_7^2 + pz_7^2} = \sqrt{hx_7^2 + hy_7^2}. \tag{14}$$

Thus, for the elevation angle ϕ

$$\cos \phi = \frac{\{hx_7, hy_7, 0\} \cdot \{hx_7, hy_7, hz_7\}}{\|\{hx_7, hy_7\}\| \|\{hx_7, hy_7, hz_7\}\|} = \frac{q_7^2}{q_7 r_7} = \frac{q_7}{r_7}. \tag{15}$$

Likewise, we have for the azimuth angle θ

$$\cos \theta = \frac{\{fx_7, 0, 0\} \cdot \{hx_7, hy_7, 0\}}{\|\{fx_7, 0, 0\}\| \|\{hx_7, hy_7, 0\}\|} = \frac{fx_7 hx_7}{(\|fx_7\|)(q_7)}. \tag{16}$$

But since $fx_7 < 0$, then $\|fx_7\| = -fx_7$ and hence

$$\cos \theta = \frac{-hx_7}{q_7}. \tag{17}$$

For the bearing angle ψ

$$\begin{aligned} \cos \psi &= \frac{\{fx_7, 0, 0\} \cdot \{hx_7, hy_7, hz_7\}}{(\|\{fx_7, 0, 0\}\|)(\|\{hx_7, hy_7, hz_7\}\|)} \\ &= \frac{fx_7 hx_7}{(\|fx_7\|)(r_7)}. \end{aligned} \tag{18}$$

Once again since $fx_7 < 0$ we have $\|fx_7\| = -fx_7$ so that we arrive at the simplified form

$$\cos \psi = \frac{-hx_7}{r_7}. \tag{19}$$

From algebraically manipulating these cosine expressions for the angle variables it can be seen that

$$\begin{aligned} \cos \psi &= \frac{-hx_7}{r_7} = \frac{-hx_7 q_7}{q_7 r_7} = \left(\frac{q_7}{r_7}\right) \left(\frac{-hx_7}{q_7}\right) \\ &= \cos \phi \cos \theta. \end{aligned} \tag{20}$$

Now we can evaluate these angles using the inverse trigonometric arccos function, but with caution since the angles they generate are multivalued with period 2π . Furthermore, there is the additional complication that for any angle ω there is the trigonometric relationship $\cos(\omega) = \cos(-\omega)$.

There is a slight complication in evaluating the elevation angle because the rotation sense from the azimuth plane will be counterclockwise if $hz_7 > 0$. Therefore, the angle itself is also positive-valued. However, the rotation sense will be clockwise if $hz_7 < 0$ so that the angle is also negative-valued. Thus, we need to incorporate the multiplicative factor $\frac{hz_7}{\|hz_7\|}$ which reflects the sign of hz_7 , as a coefficient for the absolute value of the arccos term. Consequently the evaluation of ϕ becomes

$$\begin{aligned} \phi &\equiv \left(\frac{hz_7}{\|hz_7\|}\right) \left|\arccos(\cos \phi)\right| \\ &= \left(\frac{hz_7}{\|hz_7\|}\right) \left|\arccos\left(\frac{q_7}{r_7}\right)\right|. \end{aligned} \tag{21}$$

In the cases of the azimuth and bearing angles, if the pursuer position is below the $\{x_7, z_7\}$ plane, (i.e., $hy_7 < 0$), then there are counterclockwise rotations of the negative x_7 axis from the vertex at the target in order to obtain directional alignment with the pursuer displacement vector, thus producing positive angle values for θ and ψ . Conversely, if $hy_7 > 0$, then the rotation of the negative x_7 axis at the target needed to align with the pursuer displacement vector is clockwise so that the values for θ and ψ are negative. To account for this there needs to be a multiplicative factor in the evaluations of θ and ψ that incorporates the opposite sign from that of hy_7 , i.e., $-\frac{hy_7}{\|hy_7\|}$, as a coefficient for the absolute value of the arccos term.

Therefore, we evaluate the azimuth angle θ as

$$\theta \equiv -\frac{hy_7}{\|hy_7\|} \left|\arccos\left(\frac{-hx_7}{q_7}\right)\right| \tag{22}$$

and the bearing angle ψ as

$$\psi \equiv -\frac{hy_7}{\|hy_7\|} \left|\arccos\left(\frac{-hx_7}{r_7}\right)\right|. \tag{23}$$

References

1. Samuel M, Hussein M, Mohamad MB (2016) A review of some pure-pursuit based path tracking techniques for control of autonomous vehicle. *Int J Comput Appl* 135(1):35–38
2. Scharf L, Harthill W, Moose P (1969) A comparison of expected flight times for intercept and pure pursuit missiles. *IEEE Trans Aerosp Electron Syst* 4:672–673
3. Baddeley A, Logie R, Bressi S, Della Sala S, Spinnler H (1986) Dementia and working memory. *Quart J Exp Psychol* 38A:603–618
4. Heitger MH, Anderson TJ, Jones RD, Dalrymple-Alford JC, Frampton CM, Ardagh MW (2004) Eye movement and visuomotor arm movement deficits following mild closed head injury. *Brain* 127(3):575–590
5. Soliveri P, Brown RG, Jahanshahi M, Caraceni T, Marsden CD (1997) Learning manual pursuit tracking skills in patients with Parkinson's disease. *Brain* 120(8):1325–1337
6. Park S, Spirduso W, Eakin T, Abraham L (2018) Force and directional force modulation effects on accuracy and variability in low-level pinch force tracking. *J Motor Behav* 50(2):210–218
7. Parker MG, Tyson SF, Weightman AP, Abbott B, Emsley R, Mansell W (2017) Perceptual control models of pursuit manual tracking demonstrate individual specificity and parameter consistency. *Atten Percept Psychophys* 79(8):2523–2537. <https://doi.org/10.3758/s13414-017-1398-2>
8. Vaillancourt DE, Newell KM (2003) Aging and the time and frequency structure of force output variability. *J Appl Physiol* 94(3):903–912

9. Huang Y, Yang Q, Chen Y, Song R (2017) Assessment of motor control during three-dimensional movements tracking with position-varying gravity compensation. *Front Neurosci*. <https://doi.org/10.3389/fnins.2017.00253>
10. Li K, Nataraj R, Marquardt TL, Li Z-M (2013) Directional coordination of thumb and finger forces during precision pinch. *PLoS ONE* 8(11):e79400. <https://doi.org/10.1371/journal.pone.0079400>
11. Vo B, Vo B, Cantoni A (2008) Bayesian filtering with random finite set observations. *IEEE Trans Signal Process* 56(4):1313–1326
12. Yan J, Pu W, Zhou S, Liu H, Bao Z (2020) Collaborative detection and power allocation framework for target tracking in multiple radar system. *Inf Fusion* 55:173–183
13. Pew RW (1974) Levels of analysis in motor control. *Brain Res* 71:393–400
14. Liu X, Tubbesing SA, Aziz TZ, Miall RC, Stein JF (1999) Effects of visual feedback on manual tracking and action tremor in Parkinson's disease. *Exp Brain Res* 129(3):477–481
15. Raab M, de Oliveira RF, Schorer J, Hegele M (2013) Adaptation of motor control strategies to environmental cues in a pursuit-tracking task. *Exp Brain Res* 228(2):155–160
16. Lewis MM (2014) Effects of varying force levels and combinations of force application and release during an isometric pinch force task. Master's thesis, The University of Texas at Austin, Austin, TX
17. Spirduso WW, Francis K, Eakin T, Stanford C (2005) Quantification of manual force control and tremor. *J Motor Behav* 37(3):197–210
18. Willmott C, Matsuura K (2006) On the use of dimensioned measures of error to evaluate the performance of spatial interpolators. *Int J Geogr Inf Sci* 20:89–102

Publisher's Note Springer Nature remains neutral with regard to jurisdictional claims in published maps and institutional affiliations.